6th International Conference on Silicon Photovoltaics, SiliconPV 2016

The effect of phosphorus diffusion gettering on recombination at grain boundaries in HPMC-Silicon wafers

Marie S. Wiig[a]*, Krzysztof Adamczyk[b], Halvard Haug[a], Kai E. Ekstrøm[b], Rune Søndenå[a]

[a]Institute for Energitechnology, Instituttveien 18, 2007 Kjeller, Norway
[b]Norwegian University for Science and Technology, Alfred Getz vei 2, 7491 Trondheim, Norway

Abstract

The influence of phosphorus diffusion gettering on recombination at grain boundaries has been studied in a commercially cast high performance multicrystalline silicon block. Wafers from four different heights have been studied with high resolution photoluminescence-imaging. The recombination at grain boundaries was studied from linescans perpendicular to the grain bounaldary of interest. The change in recombination activity at grain boundaries after gettering has been correlated with grain orientation measured by electron backscatter diffraction and classified according to Brandon criterion. The relative change in carrier lifetime after gettering depends on the height in the cast, and is very sensitive to the injection level. Iron concentrations were also found from photoluminescence-imaging of iron in Fe_i and FeB states, respectively. After gettering recombination grain boundaries in the middle section of the ingot has become strongly recombination active. Fe_i has been efficiently removed and no longer constitute the main recombination path at any height.

Keywords: Photoluminesce-imaging, grain boundary recombination, HPMC-Si, EBSD, \

1. Introduction

   The performance of multicrystalline silicon (mc-Si) solar cells is limited by impurities, crystal defects and interactions thereof[1-3]. Crystal defects such as grain boundaries and dislocations are easily decorated with impurity species, forming recombination active defects in the material[4-6]. Dislocation clusters are especially

---

* Corresponding author. E-mail address: Marie.Syre.Wiig@ife.no

detrimental to the minority carrier lifetime in conventional mc-Si as dislocations multiply and grow during solidification[7-9]. In addition phosphorus diffusion gettering (PDG) has proven to be less effective in removing impurities trapped by these crystal defects[10].

Recent years the industry has moved toward new methods for casting multicrystalline silicon ingots. High performance multicrystalline silicon (HPMC-Si) denotes mc-Si with improved material properties [11]. A seed layer or seed structure is typically used to control the initial growth of the ingot in order to avoid much of the dislocation growth[11, 12]. As a result HPMC-Si typically has smaller grain sizes, but less dislocations than conventional mc-Si[13]. However, smaller grain sizes alone is not beneficial for the minority carrier lifetime, as an increase in grain boundaries is implied. Improved understanding of the electrical properties of grain boundaries during the different solar cell processing steps is therefore important as it allows for further improvement of the final cell performance.

Phosphorus diffusion gettering is routinely used in solar cell processing to remove metallic impurities, and to form the emitter. PDG is commonly known to improve the lifetime of multicrystalline silicon[14], however, recent publications have shown a decrease in average lifetime despite the removal of metallic impurities during the gettering process[9, 15]. Increased recombination after PDG can in some cases be reversed by H-passivation after SiN-fireing[6, 16].

In the present work the effect of phosphorus diffusion gettering on the recombination activity of grain boundaries in commercially available HPMC-Si wafers is studied by investigating the photoluminescence of both passivated and non-passivated wafers. Gettered and ungettered wafers are compared in order to better understand the local effects on the recombination activity. Grain boundaries are classified using electron backscatter diffraction (EBSD).

2. Experimental

Four wafers from four positions in a commercially cast p-type high performance multicrystalline silicon block were studied. The processing of neighbouring wafers from each height is illustrated in Figure 1. Four wafers from each position were etched to remove saw damage. This etched state will later be referred to as ungettered. Phosphorus diffusion gettering at 835°C was then carried out on two wafers from each position, followed by etching to remove the diffused emitter. The samples were then split in two batches were one received double side surface passivation by hydrogenated amorphous silicon, the other half were kept unpassivated.
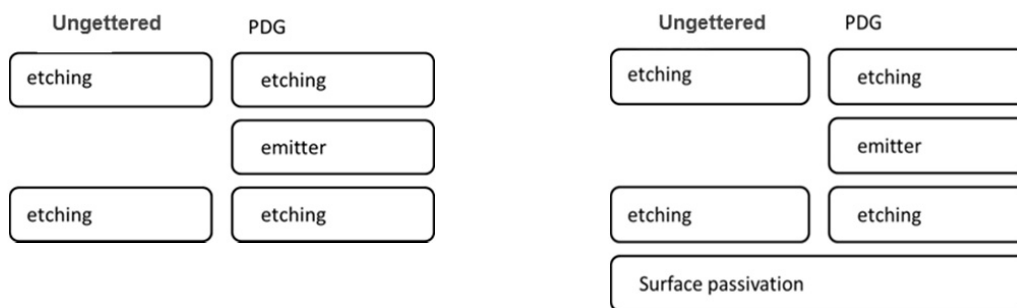
Fig. 1. Illustration of how the four samples from each height is processed.

Band-to-band photoluminescence (PL) imaging shows the local recombination activity with high resolution. From unpassivated images one can observe sharp features where strong recombination centres are present. The images show a 2x2 cm^2 area captured with a high magnification lens (20 pixels/mm) which resolves fine features not visible when imaging the full wafer. The recombination activity at and in the vicinity of grain boundaries has been studied from linescans perpendicular to the GB of interest in PL-images. For material with high lifetime and good surface passivation the diffusion length of carriers is sufficient to cause a smearing of the PL-signal, due to transport of carriers from high lifetime to low lifetime regions. The PL signal scales with excess carrier concentration ($\triangle$n) which is the sum of the recombination current (U) and net carrier diffusion. In order to eliminate

this effect, and locate the region where the recombination actually takes place, unpassivated samples were evaluated. In this case the surface recombination is very high eliminating the contribution from net diffusion of carriers, beyond the wafer thickness.

Grain orientations have been found by EBSD and grain boundary degree of fit has been identified according to Brandon criterion.

PL imaging calibrated by harmonically modulated photoluminescence[17] in combination with metastable defect imaging provides images of the concentration of interstitial iron[18]. These measurements were performed at Fraunhofer ISE.

3. Results and Discussion

3.1. Lifetime and Fe-concentration

The mean lifetime measured by Quasi Steady State Photoconductance (QSSPC) along the height of the block before and after PDG is show in Figure 2. After PDG the lifetime in the top and bottom section with initially very low lifetimes improved. However, in the middle section of the block the mean lifetime slightly decreased after PDG. Iron imaging of wafers from the same positions showed a reduction of Fe_i concentration in top and bottom with approximately two orders of magnitude, and one order of magnitude in the middle section. In the ungettered top and bottom wafers almost 90% of the carrier recombination was due to Fe_i. In the middle section this fraction was around 35-50%, see more details in Table 1. After PDG Fe_i was no longer the dominating recombination path at any height.
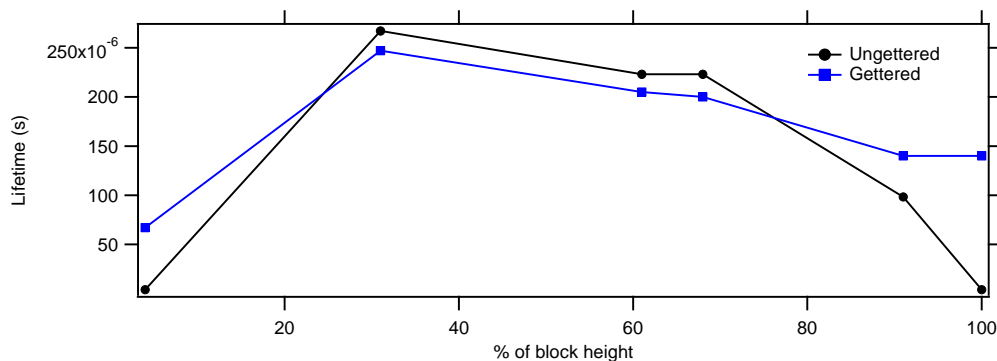

Fig. 2. QSSPC lifetime at 1e15 cm-3 (or maximum injection level) as a function of height in the block.

Table 1: Iron concentrations measured by metastable defect imaging photoluminescence imaging by calibrated by harmonically modulated photoluminescence. Calculated recombination fraction due to Fe_i.

	% Fe_i recomb. gettered	% Fe_i recomb. Ungettered	Fe_i gettered	Fe_i ungettered
Bottom	8.8%	87%	1.3e10	3e12
Lower center	2.7%	37%	2.6e9	3.4e10
Upper center	4.8%	48%	5.4e9	5.2e10
Topp	3.6%	88%	6.2e9	2.2e12

3.2. Bottom of ingot

PL-images of unpassivated samples do not suffer from smearing, which occur in PL-images of passivated samples with high lifetime. Figure 3 show distinct difference in recombination at and around the grain boundaries

before and after PDG. The ungettered bottom wafer had highly recombination active grain boundaries in the ungettered state surrounded by a region of higher lifetime, seen as a bright region surrounding the GB in the PL-image. After PDG gettering, most GB's are still strong recombination centers but the bright region has vanished.
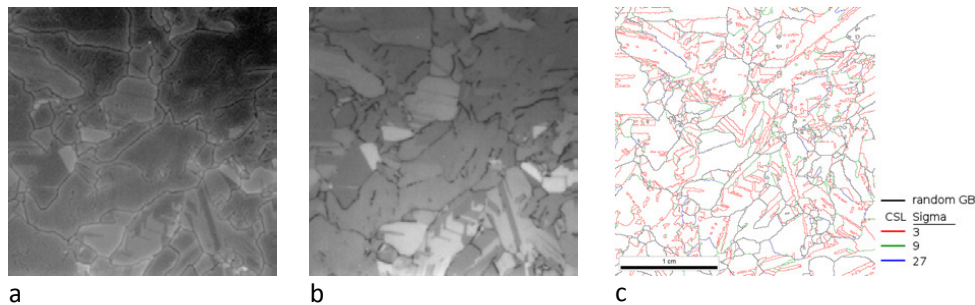

Fig. 3. High magification PL-image of an unpassivated a) ungettered and b) gettered wafer from the bottom section of the cast (4% of ingot height). EBSD map from same wafer position is shown in c).

A linescan perpendicular to a GB in the bottom wafer is shown in Figure 4. The average Fe_i concentration in this bottom wafer was reduced by two orders of magnitude and the overall lifetime after PDG increased.
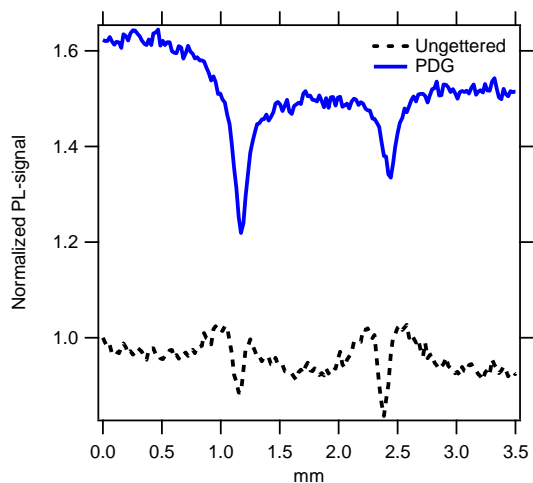

Fig. 4. Linescan from PL-image perpendicular to a GB. The black/dashed line represent the ungettered wafer.

The increased PL-signal next to the GB after PDG corresponds well with a denuded zone formed around the GB due internal gettering of impurities to precipitates formed during cooling of the ingot[5]. Grain boundaries are known as preferred nucleation sites for iron precipitation, there is a smaller barrier to growth of already existing precipitates, compared to the nucleation of new precipitates[19]. Attributing this denuded zone to diffusion of iron also agree well with profiles from high resolution iron imaging[5, 20]. The highly recombination active region observed in the centre of the grain boundary is likely due to existence of Fe precipitates. This phenomenon is only observed in the bottom region with high iron concentration. After PDG the denuded zone around the GB vanished. In literature EBIC studies has also revealed a denuded zone around moderately and heavy contaminated Σ27 and RA grain boundaries[21]. Σ3 GB's were inactive and unaffected by PDG, this has also been reported previously by others[22].

3.3. Middle section of ingot

Wafers from these centre positions represent typical properties in the major part of the ingot. Opposed to the highly recombining GB's in the ungettered bottom wafer, no strongly recombining grain boundaries are visible in the ungettered wafers from 30% and 60% of the block height, Figure 5. After PDG recombination at some of the GB's has been activated. Most of the strongly activated GB's have been classified as random angle (RA) and a few as Σ27. The inactive grain boundaries in the ungettered material may imply that there are no preexcisting precipitation sites around the GB's, resulting in a larger number of small precipitates and strong activation of recombination after PDG[23]. As in the bottom wafer GB's classified as Σ3 are inactive both before and after PDG.
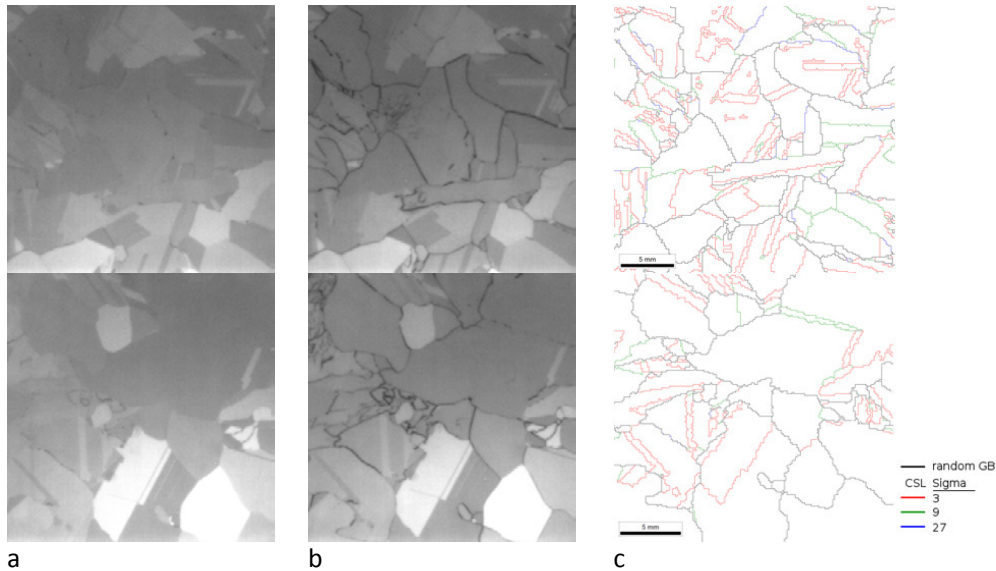

Fig. 5. High magification PL-image of unpassivated a) ungettered and b) gettered wafer from the middle section of the cast (Upper row 30% and lower row 60% of ingot height). EBSD map from same ingot height is shown in c).

A linescan for such an activated GB is shown in Figure 6. After PDG a previously inactive grain boundary has become strongly recombination active, as previously also reported by Rinio[6] and Geerlings[15]. Figure 6 shows the grain boundary as an abrupt decrease in the PL signal where it appears as a step in the PL signal between two adjacent grains in the ungettered sample. The higher levels of the left grain compared to the right is due to higher reflectivity, surface recombination velocities or light emission for different grain orientations. Σ3 grain boundaries between grains with equal bulk signal cannot be observed from the PL signal. Increased recombination in vicinity of GB's after PDG has previously been attributed out-diffusion of impurities, also referred to as bleeding or poisoning of the bulk silicon, from the grain boundaries during the high temperature emitter in-diffusion process[6]. Or it can be due to increased recombination activity of certain GB's after PDG[15, 19] due to precipitation.
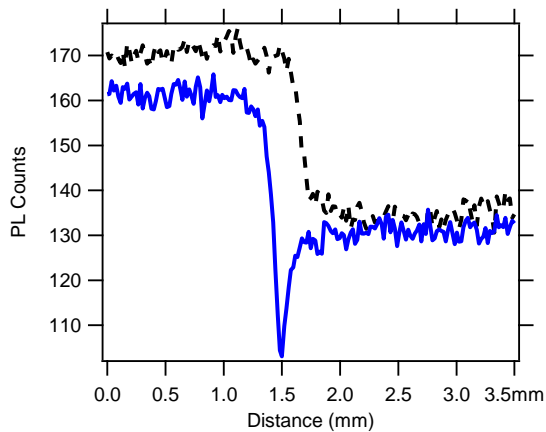
Fig. 6.PL signal at a RA grain boundary. Dashed line show ungettered and solid line is after PDG.

Figure 7b show coincidence of the inflection point (d^2y/dx =0) of two peak fitted PL-signals (Figure 7a) of a grain boundary which were recombination active already in the ungettered state. The coincidence of the inflection point for these two profiles indicate that the width of the recombination active GB is unaffected by PDG. This indicates that the increased recombination after PDG in this case is rather due to increased precipitate density than out-diffusion of supersaturated dissolved impurity atoms from the extended defect[6, 24]. The rapid cooling after PDG freezes the small precipitates, which results in larger recombination activity than a few large precipitates formed during slow cooling of the ingot[15].
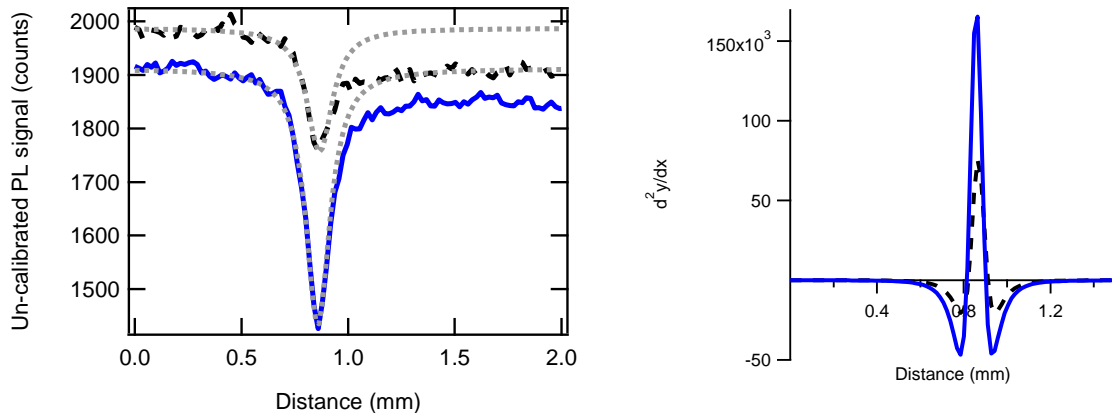

Fig. 7. (a) Uncalibrated PL signal at GB. Solid line PDG and dashed line ungettered samples. The dotted lines are peak fitted curves with respect to the left grain. Double derivatives of the peak fitted signals are shown in (b).

3.4. Upper section of ingot

In the top wafer the same GB's are recombination active both before and after PDG. Similar to all the samples from lower heights Σ3 GB's are inactive and unaffected by PDG. Only a few inactive Σ9 GB and no long Σ27 GB's were detected. Even though the iron concentration is comparable to the bottom section, there is no sign of a denuded

zone which was observed in the bottom wafer. This can be because the top of a cast is allowed shorter time for diffusion of impurities after it has solidified.
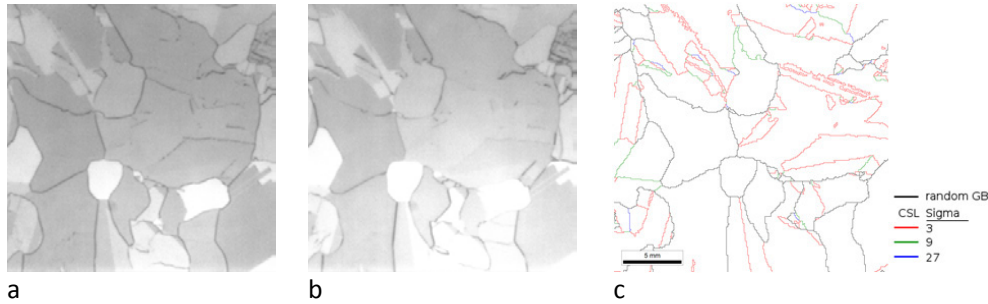

a   b   c

Fig. 8. High magification PL-image of an un-passivated a) ungettered and b) gettered wafer from the upper section of the cast (100% of wafered block height). EBSD map from same wafer position is shown in c).

3.5. Injection dependence of GB recombination

Recombination strength and injection dependence of the recombination processes has been studied on double side passivated wafers from the middle section of the ingot.

Fe_i was efficiently removed after PDG, and the typical crossover point in the QSSPC signature of Fe_i and FeB disappeared. Still the PL signal from the bulk grains measured after PDG was reduced. One reason for measuring a lower lifetime with QSSPC calibrated PL after PDG is strong recombination of carriers at the grain boundaries and diffusion of carriers toward this sink. This reduces the number of free carriers far into the bulk grains on samples with good surface passivation. On HPMC-Si with a small to moderate grain size this may dominate the measured lifetime after PDG, where real bulk lifetime values are never reached. This strong gradient in the injection level toward the GB's makes QSSPC calibration of the PL-signal to lifetime after PDG inaccurate. QSSPC calibration of PL-images depends on an injection dependent calibration constant which is not globally valid for strongly inhomogeneous samples. To study the injection dependent recombination uncalibrated images were acquired at different illumination flux. The recombination activity after PDG as a function of illumination intensity has been extracted from the uncalibrated PL-signal divided by illumination flux for bulk and GB's separately in Figure 9. After PDG there is a clear activation of recombination at the grain boundary relative to the neighboring grains. There is also an increased dissimilarity between different grains. However, whether there is an increase or decrease in recombination activity in the grains after PDG with respect to the ungettered state, depends on the injection conditions. At moderate to high injection there is an increase in the recombination activity after PDG, Figure 9c). However, at low injection the lifetime appears to improve, Figure 9b).

After PDG the recombination strength of the different grains and grain boundaries varies, but the dependence on illumination intensity is the same. This indicates that the recombination mechanism which limits the carrier lifetime is the same in bulk and at active GB's, but the concentration may vary depending on location.
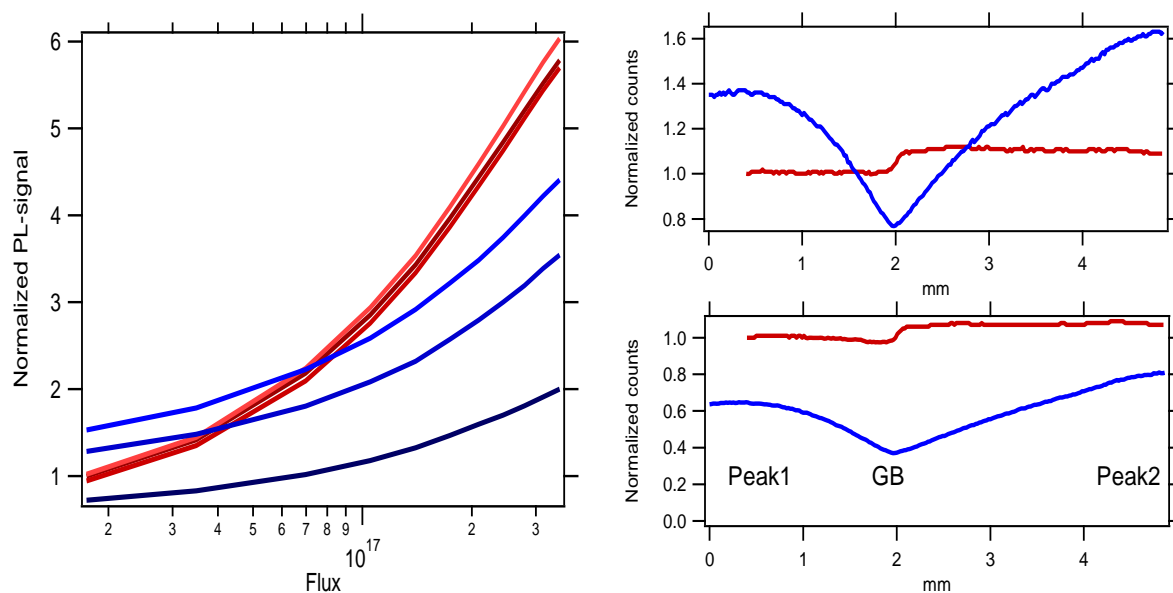
Fig. 9. (a) Normalized PL-signal (against Peak1 ungettered) vs illumination flux for Peak1, GB and Peak2. red) ungettered and blue) PDG. b) Linescans across a the grain boundary b) 1.7e16 and c) 2.1e17 Photons/cm2

The Fe_i concentrations are reduced by 90% or more by phosphorus diffusion gettering. If the Fe_i was the only recombination mechanism influenced by PDG, one would from Shockley-Read-Hall (SRH) recombination theory expect reduced injection dependence and improved lifetime after PDG. However, we observe a crossover point between the injection dependent recombination before and after PDG, Figure 9a. According to this an additional recombination mechanism has been activated after PDG, and it is active both in bulk and at GB's. This is in agreement with findings of Scott et al.[25] also ruling out iron as a cause for reduced lifetimes after gettering at increasing temperatures. It is currently not clear what this additional recombination mechanism is, however, dissolution of metal impurities with lower diffusivity and solid solubility[25] or precipitation within the grains[26] are possible candidates. Also in the ungettered state the recombination is not completely dominated by Fe_i as about half of the recombination processes are through other paths, of which some may be enhanced after PDG.

We observe a reduced injection dependence of the recombination at GB's after PDG. SiO et al.[23, 27] quantified recombination at GB's according to surface recombination velocity. Contrary to our finding they found two classes of GB's one with increased in injection dependence after PDG and one which had similar injection dependence before and after.

Recombination at GB's after PDG can be reduced after subsequent H-passivation during SiN-fireing[15, 16]. This may reduce the severity of GB activation on the final solar cell. The effect of H-passivation has not been part of this study.

4. Conclusion

The influence of PDG on recombination activity at the GB's strongly depends on the height in the cast. For all positons Σ3 CSL grain boundaries were unaffected by PDG. Grain boundaries in the bottom wafer were surrounded by a higher lifetime region, denuded zone. This was completely removed after PDG and the overall lifetime improved.

In the middle section of the ingot a large number of RA grain boundaries inactive in the ungettered state became recombination active after PDG gettering. Even though the recombination strength changed, the width of an initially recombination active GB remained constant after phosphorus diffusion. For the wafers from the middle section strong recombination at the grain boundaries caused strong gradients in the carrier density in the sample and

enhanced diffusion toward the grain boundaries. These locally large gradients in carrier concentrations also made QSSPC calibrated lifetime less accurate and evaluating recombination from uncalibrated PL signal were preferred. After PDG recombination due to Fe_i has been reduced, however a new recombination path has been activated. This recombination path has the same injection dependence both on GB's and in bulk grains.

In the top wafer the same GB's were recombination active both before and after PDG.

Carrier recombination due to Fe_i is no longer the main lifetime limiting recombination path after PDG at any height. Only the top and bottom wafer positions with initially high iron concentration showed reduced recombination activity after PDG.

Acknowledgements

References

[1] Coletti G, Sensitivity of state-of-the-art and high efficiency crystalline silicon solar cells to metal impurities, Progress in Photovoltaics: Research and Applications, 2013:21: 1163-1170.
[2] Kveder V, Kittler M, Schröter W, Recombination activity of contaminated dislocations in silicon: A model describing electron-beam-induced current contrast behavior, Physical Review B, 2001:63: 115208.
[3] Schindler F, Michl B, Schon J, et al., Solar Cell Efficiency Losses Due to Impurities From the Crucible in Multicrystalline Silicon, Photovoltaics, IEEE Journal of, 2014:4: 122-129.
[4] Buonassisi T, Istratov AA, Peters S, et al., Impact of metal silicide precipitate dissolution during rapid thermal processing of multicrystalline silicon solar cells, Applied Physics Letters, 2005:87: 121918.
[5] Liu AY, Walter D, Phang SP, et al., Investigating Internal Gettering of Iron at Grain Boundaries in Multicrystalline Silicon via Photoluminescence Imaging, Photovoltaics, IEEE Journal of, 2012:2: 479-484.
[6] Rinio M, Yodyungyong A, Keipert-Colberg S, et al., Recombination in ingot cast silicon solar cells, physica status solidi (a), 2011:208: 760-768.
[7] Ryningen B, Stokkan G, Kivambe M, et al., Growth of dislocation clusters during directional solidification of multicrystalline silicon ingots, Acta Materialia, 2011:59: 7703-7710.
[8] Stokkan G, Hu Y, Mjøs Ø, et al., Study of evolution of dislocation clusters in high performance multicrystalline silicon, Solar Energy Materials and Solar Cells, 2014:130: 679-685.
[9] Søndenå R, Gjessing J, Angelskår H, et al., Effect of dislocations on the electrical response of mulicrystalline silicon solar cells. , in: 28th European Photovoltaic Solar Energy Conference and Exhibition, Paris, 2013.
[10] Bentzen A, Holt A, Overview of phosphorus diffusion and gettering in multicrystalline silicon, Materials Science and Engineering: B, 2009:159–160: 228-234.
[11] Yang YM, Yu A, Hsu B, et al., Development of high-performance multicrystalline silicon for photovoltaic industry, Progress in Photovoltaics: Research and Applications, 2015:23: 340-351.
[12] Wong YT, Hsu C, Lan CW, Development of grain structures of multi-crystalline silicon from randomly orientated seeds in directional solidification, Journal of Crystal Growth, 2014:387: 10-15.
[13] Ekstrøm K, Stokkan G, Autruffe A, et al., Microstructure of multicrystalline silicon seeded by polysilicon chips and fluidized bed reactor granules, Journal of Crystal Growth, 2016: 95-100.
[14] Gindner S, Karzel P, Herzog B, et al., Efficacy of Phosphorus Gettering and Hydrogenation in Multicrystalline Silicon, Photovoltaics, IEEE Journal of, 2014:4: 1063-1070.
[15] Geerligs LJ, Komatsu Y, Rover I, et al., Precipitates and hydrogen passivation at crystal defects in n- and p-type multicrystalline silicon, J. Appl. Phys., 2007:102: 093702-093702-093709.
[16] Karzel P, Ackermann M, Gröner L, et al., Dependence of phosphorus gettering and hydrogen passivation efficacy on grain boundary type in multicrystalline silicon, J. Appl. Phys., 2013:114: 244902.
[17] Giesecke JA, Schubert MC, Michl B, et al., Minority carrier lifetime imaging of silicon wafers calibrated by quasi-steady-state photoluminescence, Solar Energy Materials and Solar Cells, 2011:95: 1011-1018.
[18] Macdonald D, Tan J, Trupke T, Imaging interstitial iron concentrations in boron-doped crystalline silicon using photoluminescence, J. Appl. Phys., 2008:103: 073710.
[19] Buonassisi T, Istratov AA, Pickett MD, et al., Chemical natures and distributions of metal impurities in multicrystalline silicon materials, Progress in Photovoltaics: Research and Applications, 2006:14: 513-531.

[20] Schubert MC, Habenicht H, Warta W, Imaging of Metastable Defects in Silicon, Photovoltaics, IEEE Journal of, 2011:1: 168-173.

[21] Chen J, Sekiguchi T, Yang D, et al., Electron-beam-induced current study of grain boundaries in multicrystalline silicon, J. Appl. Phys., 2004:96: 5490-5495.

[22] Takahashi I, Usami N, Mizuseki H, et al., Impact of type of crystal defects in multicrystalline Si on electrical properties and interaction with impurities, J. Appl. Phys., 2011:109: 033504.

[23] Sio HC, Phang SP, Trupke T, et al., Impact of Phosphorous Gettering and Hydrogenation on the Surface Recombination Velocity of Grain Boundaries in p-Type Multicrystalline Silicon, IEEE Journal of Photovoltaics, 2015:5: 1357-1365.

[24] Habenicht H, Riepe S, Schultz W, et al., Out-diffusion of metal from grain boundaries in multicrystalline silicon during thermal processing, in: EUPVSEC, Milan, Italy, 2007.

[25] Scott SM, Hofstetter J, Morishige AE, et al., Sacrificial high-temperature phosphorus diffusion gettering process for lifetime improvement of multicrystalline silicon wafers, in: Photovoltaic Specialist Conference (PVSC), 2014 IEEE 40th, 2014, pp. 3014-3016.

[26] Liu AY, Macdonald D, Precipitation of iron in multicrystalline silicon during annealing, J. Appl. Phys., 2014:115: 114901.

[27] Sio HC, Trupke T, Macdonald D, Quantifying carrier recombination at grain boundaries in multicrystalline silicon wafers through photoluminescence imaging, J. Appl. Phys., 2014:116: 244905.